Heating from continuous number density measurements in optical lattices

Yariv Yanay and Erich J. Mueller
Laboratory of Atomic and Solid State Physics, Cornell University, Ithaca, New York 14850, USA
(Received 20 May 2014; published 7 August 2014)

We explore the effects of continuous number density measurement on atoms in an optical lattice. By integrating a master equation for quantum observables, we calculate how single-particle correlations decay. We consider weakly and strongly interacting bosons and noninteracting fermions. Even in the Mott regime, such measurements destroy correlations and increase the average energy, as long as some hopping is allowed. We explore the role of spatial resolution and find that the heating rate is proportional to the amount of information gained from such measurements.

DOI: 10.1103/PhysRevA.90.023611 PACS number(s): 03.75.Lm, 67.85.Hj

I. INTRODUCTION

One of the most important recent advances in cold atom experiments is single-site resolved imaging in optical lattices [1–4]. Presently these techniques are destructive and do not directly yield dynamical information. While backaction from measurement is inherent to quantum mechanics, a less destructive local probe is desirable, as it would enable whole classes of new experiments [5]. Here we explore the ultimate limits on such a program, calculating how correlations evolve during ideal continuous local-density measurements. We quantify the heating in weakly and strongly interacting gases.

Quantum backaction arises when the system's energy eigenstates and the measurement operator do not commute. While this backaction can be a useful resource [6–12], more often it leads to unwanted heating or decoherence [13–17]. We consider measuring the local density of atoms in a lattice. Such a measurement localizes individual atoms to single sites, projecting their wave functions to superpositions of momentum states. As noted by Poletti *et al.* [18], in the long-time limit, this results in an infinite temperature system where all kinetically accessible many-body Fock states are equally likely.

We quantify the approach to this steady state using a master equation for the nonunitary evolution of the density matrix and observables. In the weakly interacting limit, where atoms are highly delocalized, off-diagonal elements of the single-particle correlation function fall off exponentially with time. In the strongly interacting limit, where number density is nearly a good quantum number, we find slower evolution: an exponential stage where quasiparticle momenta are scrambled is followed by a slow proliferation of excitations and a parallel decay in correlations.

This heating arises even if the measurement photons are never detected. Thus our formalism is nearly identical to that used by others [18–25] to study spontaneous off-resonant light scattering in an optical lattice. Other works approached the subject using different formalisms [26–30].

Our principal results come from from applying variants of the Bogoliubov approximation and calculating the time dependence of single-particle correlation functions. Such approaches work well in both the weakly and strongly interacting limits but do not accurately describe intermediate coupling strength [31]. Previous works used one-dimensional numerical techniques or assumed slow photon scattering rates. Our approximations apply to three-dimensional systems and do not restrict the scattering rate. Our results are consistent with previous studies and in many places extend our understanding. For example, the doublon-holon picture we present in Sec. IV gives a clear explanation of the two time scales that have been previously observed in the Mott regime [18] and allows us to quantify the decay rates associated with each.

Our paper is organized as follows. In Sec. II, we introduce our model and the master equations used to calculate the evolution of the system. From the form of the expressions we make some general observation about the evolution of momentum states and single-particle correlations. In Sec. III, we use a Bogoliubov approach to integrate the master equations for weakly interacting bosons. In Sec. IV we extend these calculations to the Mott regime through a doublon-holon formalism. Finally, in Sec. V we consider the use of longer-wavelength light in measurement, exploring the tradeoff between information extracted from the system and the heating caused by measurement.

II. MODEL

We model the optical lattice system with the single-band Hubbard model:

$$\begin{aligned}\hat{H} &= -J\sum_{\langle i,j\rangle}(\hat{a}_i^\dagger\hat{a}_j+\hat{a}_j^\dagger\hat{a}_i)\\ &\quad+\sum_i\frac{U}{2}\hat{n}_i(\hat{n}_i-1)-(\mu-2JD)\hat{n}_i\\ &=\sum_k(J\epsilon_k-\mu)\hat{n}_k+\frac{U}{2}\sum_i\hat{n}_i(\hat{n}_i-1),\end{aligned}\tag{1}$$

where $\hat{a}_i$ ($\hat{a}_i^\dagger$) is the annihilation (creation) operator at site i; $\langle i,j\rangle$ are nearest-neighbor sites i and j; $\hat{n}_i=\hat{a}_i^\dagger\hat{a}_i$ is the occupation operator at site i; $\hat{n}_k=\hat{a}_k^\dagger\hat{a}_k$ is the occupation of the momentum mode $\boldsymbol{k}$; and $2D$ is the number of nearest neighbors per site. J, U, and μ are the hopping energy, interaction energy, and chemical potential, respectively. Here we define $\hat{a}_k=\frac{1}{\sqrt{N_s}}\sum_i e^{i\boldsymbol{k}\cdot\boldsymbol{r}_i}\hat{a}_i$, summing over N_s sites at positions $\boldsymbol{r}_i$. The kinetic energy is given by $J\epsilon_k=J\sum 4\sin^2(\boldsymbol{k}\cdot\Delta\boldsymbol{r}/2)$ where the sum is over all lattice basis vectors $\Delta\boldsymbol{r}$.

We model the measurement process as an additional term of the form $\hat{H}_I = \lambda \sum_\alpha (\hat{c}_\alpha + \hat{c}_\alpha^\dagger)\hat{M}_\alpha$ where $\hat{c}_\alpha$ are annihilation operators for a set of independent zero-temperature photon baths. For single-site resolved position measurements, we take $\hat{M}_\alpha = \hat{n}_i$. We consider a more general operator in Sec. V. Following Gardiner [32] we adiabatically eliminate the density matrix of the photons to derive a master equation for $\hat{\rho}$, the density matrix of the atoms:

$$\frac{d}{dt}\hat{\rho} = i[\hat{\rho},\hat{H}] - \frac{1}{2}\gamma \sum_i [\hat{n}_i,[\hat{n}_i,\hat{\rho}]], \tag{2}$$

where we have taken λ as real and used that $\hat{n}_i$ is Hermitian. Here γ is an energy scale related to the measurement rate. It is proportional to λ and the density of photon states. A more detailed derivation is found in Ref. [19].

While the density matrix contains all information about the system, it has an exponentially large number of terms. Thus it is more convenient to work with observables such as $\hat{n}_i$ and $\hat{n}_i^2$ that are experimentally accessible. Using $\langle \hat{O}\rangle = \mathrm{Tr}[\hat{\rho}\hat{O}]$, the evolution of observables is governed by

$$\frac{d}{dt}\langle \hat{O}\rangle = i\langle [\hat{H},\hat{O}]\rangle - \frac{1}{2}\gamma \sum_i \langle [\hat{n}_i,[\hat{n}_i,\hat{O}]]\rangle. \tag{3}$$

Most of our results concern bosonic atoms, though we briefly address the case of noninteracting, spinless fermions. Much of the intuition gained carries over to interacting fermions. Regardless of statistics, each photon scattered localizes a particle, generically heating the system by increasing the kinetic energy.

Throughout, we assume a homogenous system.

A. Equations of motion for single-particle observables

The single-particle correlations can be studied in momentum space or position space. In a homogenous system, the relevant observables evolve as

$$\frac{d}{dt}\langle \hat{n}_k\rangle = -2U\frac{1}{N_s}\sum_{p,q}\mathrm{Im}[\langle \hat{a}_{p-q}^\dagger \hat{a}_{k+q}^\dagger \hat{a}_p \hat{a}_k\rangle] - \gamma(\langle \hat{n}_p\rangle - \rho), \tag{4}$$

$$\frac{d}{dt}\langle \hat{a}_i^\dagger \hat{a}_j\rangle = iU(\langle \hat{a}_i^\dagger \hat{n}_i \hat{a}_j\rangle - \langle \hat{a}_i^\dagger \hat{n}_j \hat{a}_j\rangle) - \gamma(\langle \hat{a}_i^\dagger \hat{a}_j\rangle - \rho\delta_{i,j}), \tag{5}$$

where $\rho = N_p/N_s$ is the average occupation per site. These are related by $\langle \hat{a}_i^\dagger \hat{a}_j\rangle = \frac{1}{N_s}\sum_k e^{i\boldsymbol{k}\cdot(\boldsymbol{r}_i-\boldsymbol{r}_j)}\langle \hat{n}_k\rangle$. Setting $i = j$ in Eq. 5 produces the intuitively obvious result that the average density $\rho = \langle \hat{a}_i^\dagger \hat{a}_i\rangle$ is constant.

B. Energy gain

Applying Eq. (3) to the Hamiltonian, we find irrespective of interactions

$$\frac{d}{dt}\langle E\rangle = \frac{d}{dt}\langle \hat{H}\rangle = \gamma J \sum_{\boldsymbol{k}} \epsilon_k(\rho - \langle \hat{n}_k\rangle). \tag{6}$$

The instantaneous rate of energy gain depends only on the kinetic energy in the system. It is proportional to the difference between the kinetic energy and the "infinite-temperature" kinetic energy of a system with $\langle \hat{n}_k\rangle = \rho$.

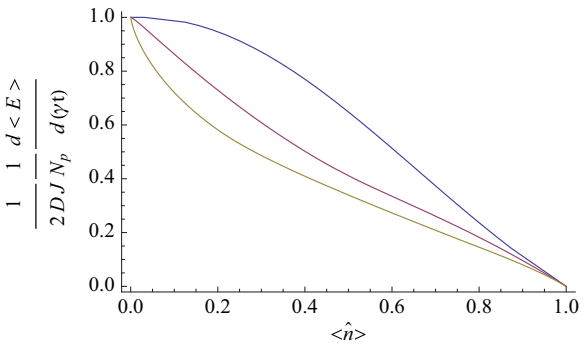

FIG. 1. (Color online) Initial rate of energy gain, $\frac{1}{2\gamma JD}\frac{1}{N_p}\frac{d}{dt}\langle E\rangle$, as a function of the filling fraction $\langle \hat{n}\rangle$ for spinless fermions. From top to bottom (blue, magenta, yellow), the figure shows the rate for a one-, two-, and three-dimensional system. For noninteracting bosons, the initial rate is always $\frac{1}{N_p}\frac{d}{dt}\langle E\rangle = 2\gamma JD$. Here J is the hopping energy, γ is the measurement rate, and D is the dimension of the system.

Equation (6) applies to both bosons and fermions. Fermions tend to have broader equilibrium momentum distributions, hence lower rates of energy gains. For free bosons at zero temperature $\langle \hat{n}_k\rangle = \delta_{k,0}N_p$, and one finds initially $\frac{1}{N_p}\frac{d}{dt}\langle E\rangle = 2\gamma J \times D$. The equivalent result for free fermions is shown in Fig. 1 as a function of filling. As $\langle n_i\rangle \to 0$, the fermionic rate approaches the bosonic rate.

This result differs from Eq. (31) in Ref. [19]. There the off-resonant light scattering from the lattice can drive atoms to high bands, while we consider measurements that are engineered to keep atoms in the lowest band. For example, in Ref. [5], Raman sideband cooling rapidly returns atoms to the lowest band.

C. Noninteracting particles

If $U = 0$, Eqs. 4 and 5 are readily integrated:

$$\begin{aligned}\langle \hat{n}_k\rangle &= (\langle \hat{n}_k\rangle_{t=0} - \rho)e^{-\gamma t} + \rho,\\ \langle \hat{a}_i^\dagger \hat{a}_j\rangle &= (\langle \hat{a}_i^\dagger \hat{a}_j\rangle_{t=0} - \delta_{ij}\rho)e^{-\gamma t} + \delta_{ij}\rho.\end{aligned} \tag{7}$$

These expressions hold for both noninteracting bosons and fermions, the only difference being initial conditions. The correlations decay exponentially with a time constant $\tau_m = 1/\gamma$ set by the measurement rate. The occupation of momentum states approaches a uniform distribution.

III. WEAKLY INTERACTING BOSONS

We extend our analysis to the weakly interacting case by a variant of the Hartree-Fock-Bogoliubov-Popov (HFBP) approach [33]. This approximation is well validated for static quantities in dimensions greater than 1. It is a gapless model which includes interactions between atoms and discards some of the coherences between noncondensed particles.

Within this formalism we calculate $\langle \hat{n}_k(t)\rangle$ for $k \neq 0$, then infer the condensate density via $\rho_c = \frac{\langle \hat{n}_0\rangle}{N_s} = \rho - \frac{1}{N_s}\sum_{\boldsymbol{k}\neq 0}\langle \hat{n}_k\rangle$. The occupation numbers evolve with Eq. (3),

where we approximate $\hat{H}$ by the HFBP Hamiltonian:

$$\hat{H}_{\mathrm{HFBP}} = -\frac{U}{2}(2\rho - \rho_c)\langle\hat{n}_0\rangle + \sum_{k\neq 0}(J\epsilon_k + U\rho_c)\hat{n}_k + \frac{1}{2}U\rho_c(\hat{a}_k\hat{a}_{-k} + \hat{a}_k^\dagger\hat{a}_{-k}^\dagger). \tag{8}$$

Evaluating the commutators in Eq. (3) yields

$$\begin{aligned}\frac{d}{dt}\langle\hat{n}_k\rangle &= -2U\rho_c\mathrm{Im}[\langle\hat{a}_k\hat{a}_{-k}\rangle] - \gamma(\langle\hat{n}_k\rangle - \rho),\\ \frac{d}{dt}\langle\hat{a}_k\hat{a}_{-k}\rangle &= -2i(J\epsilon_k + U\rho_c)\langle\hat{a}_k\hat{a}_{-k}\rangle - iU\rho_c(\langle\hat{n}_k\rangle + \langle\hat{n}_{-k}\rangle + 1)\\ &\quad - \gamma(\langle\hat{a}_k\hat{a}_{-k}\rangle + \frac{1}{N_s}\sum_p\langle\hat{a}_p\hat{a}_{-p}\rangle),\end{aligned} \tag{9}$$

whereby the equations of motion of $\langle\hat{n}_k\rangle$ are coupled to those of $\langle\hat{a}_k\hat{a}_{-k}\rangle$.

Consistent with the Popov approximation, we replace $\sum_p\langle\hat{a}_p\hat{a}_{-p}\rangle \to \rho_c$. This approximation only discards terms which vanish as $N_s \to \infty$.

These coupled equations can be perturbatively integrated for $U \ll J\epsilon_k$, yielding to first order in U/J

$$\langle\hat{n}_k\rangle \approx (\langle\hat{n}_k\rangle_{t=0} - \rho)e^{-\gamma t} + \rho - \frac{U\rho^2}{J}\frac{4J^2\epsilon_k}{\gamma^2 + 4J^2\epsilon_k^2}e^{-\gamma t}(1 - e^{-\gamma t}) + \frac{U\rho^2}{J}\frac{2\gamma[\gamma\sin^2(J\epsilon_k t) + J\epsilon_k\sin(2J\epsilon_k t)]}{\epsilon_k(\gamma^2 + 4J^2\epsilon_k^2)}e^{-2\gamma t}. \tag{10}$$

By integrating over all momenta we find the condensate density. The leading behavior coincides with Eq. (7). The deviation from this form is shown for a range of γ/J in Fig. 2. In three dimensions, this deviation is capped at $\rho_c - \rho e^{-\gamma t} \sim 0.1\frac{U\rho^2}{J}$. Thus we expect detecting it would be very difficult.

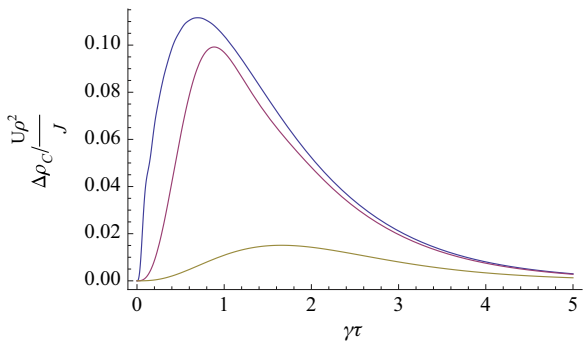

FIG. 2. (Color online) Corrections to the exponential decay of the condensate density, $\Delta\rho_c = \rho_c(t) - \rho e^{-\gamma t}$, induced by weak interactions. From top to bottom (blue, magenta, yellow) the figure shows the corrections for $\gamma/J = 0.1, 1, 5$ in a three-dimensional cubic lattice.

IV. STRONGLY INTERACTING BOSONS

The low-energy states of the $U/J \gg 1$ Bose-Hubbard model with near integer filling, $|\rho - \bar{n}| \ll 1$ for some integer $\bar{n}$, can be described by the subspace made up of states where the single site occupations are $\bar{n}, \bar{n} \pm 1$ [34]. We model this behavior by introducing "doublons" and "holons" as hard-core particles representing an occupation of one higher or one lower than the mean $\bar{n}$:

$$\hat{a}_i \to \sqrt{\bar{n}+1}\hat{d}_i + \sqrt{\bar{n}}\hat{h}_i^\dagger, \tag{11}$$

with $\hat{d}_i^2 = \hat{h}_i^2 = \hat{h}_i\hat{d}_i = 0$. The names "doublons" and "holons" are motivated by the most common case, $\bar{n} = 1$. The effective Hamiltonian becomes

$$\hat{H}_{\mathrm{DH}} = \sum_k\left[\frac{U}{2} + J\left(\sqrt{\tilde{n}^2 + \frac{1}{4}} + \frac{1}{2}\right)\varepsilon_k\right]\hat{d}_k^\dagger\hat{d}_k + \left[\frac{U}{2} + J\left(\sqrt{\tilde{n}^2 + \frac{1}{4}} - \frac{1}{2}\right)\varepsilon_k\right]\hat{h}_k^\dagger\hat{h}_k + J\tilde{n}\varepsilon_k(\hat{d}_k\hat{h}_{-k} + \hat{h}_{-k}^\dagger\hat{d}_k^\dagger), \tag{12}$$

where $\hat{d}_k, \hat{h}_k$ are related to $\hat{d}_i, \hat{h}_i$ in the same way as $\hat{a}_k$ is to $\hat{a}_i$. Here $J\varepsilon_k = J(\epsilon_k - 2D) = -2J\sum_{\Delta\boldsymbol{r}}\cos(\boldsymbol{k}\cdot\Delta\boldsymbol{r})$ is the kinetic energy and $\tilde{n} = \sqrt{\bar{n}(\bar{n}+1)}$.

This structure is similar to that in Eq. (8) with two exceptions. First, the Hamiltonian of Eq. (12) allows for the creation of doublons and holons in pairs. Second, the hard-core constraints give nonbosonic commutation relations [see Eq. (A5)]. Neglecting noncoherent summations, these relations become

$$[\hat{d}_k, \hat{d}_q^\dagger] \to \delta_{k,q}(1 - 2\hat{n}^d - \hat{n}^h), \tag{13}$$

where $\hat{n}^d = \frac{1}{N_s}\sum_k\hat{d}_k^\dagger\hat{d}_k$ is the density of doublons and $\hat{n}^h$ is the density of holons. This approximation is equivalent to a mean-field theory of the interactions.

We apply Eq. (3) to the Hamiltonian of Eq. (12), using the approximate commutation relations of Eq. (13). We decouple the equations for two-point functions from higher-order correlations by assuming

$$\langle\hat{n}^d\hat{d}_k^\dagger\hat{d}_k\rangle \to n^d\langle\hat{d}_k^\dagger\hat{d}_k\rangle \tag{14}$$

and similarly for all combinations of $\hat{n}^d, \hat{n}^h$ with $\hat{d}_k^\dagger\hat{d}_k, \hat{h}_k^\dagger\hat{h}_k$, or $\hat{d}_k\hat{h}_{-k}$. Here $n^d = \langle\hat{n}^d\rangle$.

Under these assumptions, we find a set of coupled equations for $\langle\hat{d}_k^\dagger\hat{d}_k\rangle$, $\langle\hat{h}_k^\dagger\hat{h}_k\rangle$, $\langle\hat{d}_k\hat{h}_{-k}\rangle$, and n^d, n^h. Working in the commensurate case, $\rho = \bar{n}$ and hence $n^d = n^h$, we solve these equations as detailed in the Appendix.

We find that the behavior of the system is characterized by two processes with two corresponding time scales.

The first process, occurring at a rate $1/\tau_m \sim \gamma$, involves the localization of quasiparticles when they are detected. It is illustrated by the occupation number of doublons with momentum k:

$$\langle\hat{d}_k^\dagger\hat{d}_k\rangle = [\langle\hat{d}_k^\dagger\hat{d}_k\rangle_{t=0} - n_k^d]e^{-\gamma t} + n_k^d - e^{-\gamma t}\Delta_k \times\left\{\frac{\gamma^2}{U^2}[1 - \cos(Ut)] + \frac{\gamma}{U}\sin(Ut)\right\} + O\left(\frac{J}{U}\right)^3. \tag{15}$$

Apart from the structure of the transient oscillatory term, this behavior is similar to the weakly interacting case in Eq. (10). The momentum distribution of the quasiparticles is driven to one which is slowly varying and nearly uniform:

$$\begin{aligned} n_k^d &= n^d + \Delta_k, \\ \Delta_k &= \frac{J^2}{U^2}\frac{2\tilde{n}^2(1-3n^d)^2U^2}{(1-3n^d)^2U^2+\gamma^2}(1-n^d)\left(\varepsilon_k^2-2D\right). \end{aligned} \tag{16}$$

As is implicit in the form of Δ_k, this represents a competition between the coherent creation of quasiparticles and the measurement-induced destruction of coherences.

In parallel, the measurement process results in a slow increase in the total number of quasiparticles. The rate of this process is characterized by $1/\tau_p \sim \frac{4D\tilde{n}^2J^2}{U^2+\gamma^2}\gamma$ and it is governed by the nonlinear equation of motion:

$$\begin{aligned} \frac{d}{dt}n^d = \frac{J^2}{U^2}\frac{4D\tilde{n}^2(1-3n^d)^2U^2}{(1-3n^d)^2U^2+\gamma^2}(1-n^d)\gamma \\ \times\left\{1-e^{-\gamma t}\left[\cos(Ut)+\frac{\gamma}{U}\sin(Ut)\right]+O\left(\frac{J}{U}\right)\right\}. \end{aligned} \tag{17}$$

One intuition for this growth comes from picturing the Mott insulator state as filled with virtual doublon-holon pairs. Whenever a virtual doublon or holon is imaged, the pair is converted into a real doublon and holon.

For shorter times, $\gamma t \ll (\frac{J}{U})^{-2}$, the number of excitations remains small, $n^d \ll 1$. Then the right-hand side of Eq. (17) may be integrated:

$$\begin{aligned} n^d = n^d_{t=0} + \frac{4D\tilde{n}J^2}{U^2+\gamma^2} \\ \times\left\{\gamma t - \frac{2\gamma^2}{U^2+\gamma^2}[1-e^{-\gamma t}\,\Xi(t)]+O\left(\frac{J}{U},n^d\right)\right\}, \end{aligned} \tag{18}$$

where the transient oscillations

$$\Xi(t) = \cos(Ut) - \frac{1}{2}\left(\frac{U}{\gamma}-\frac{\gamma}{U}\right)\sin(Ut) \tag{19}$$

are followed by linear growth in the excitation density.

The complete time evolution of $\langle n^d\rangle$ is plotted in Fig. 3 for typical parameters.

Within our approximations, $n^d \to \frac{1}{3}$ as long times. This is the infinite temperature limit of the model in Eq. (12): each site is equally likely to be empty, have a doublon, or have a holon. However, once n^d is of order unity, the model no longer fully describes the physics, and one must include larger fluctuation in the site occupation to fully capture the physics.

The atom correlation functions can be calculated from those of the doublons and holons. They will be short ranged, dominated by nearest-neighbor correlations,

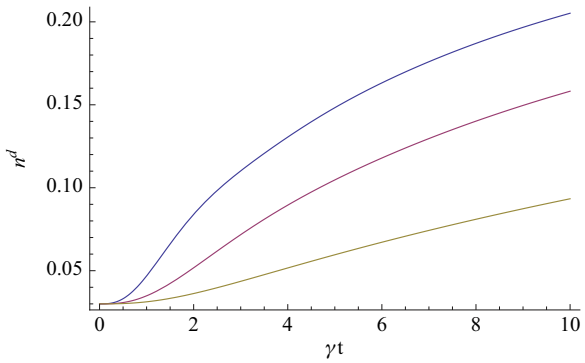

FIG. 3. (Color online) Growth in doublon density with measurement in a Mott system. At short times, the measurement process primarily scatters doublons into a uniform momentum occupation. This is followed by a growth in doublon density that is initially linear and levels off as a result of the hard-core constraints on doublon occupation. From top to bottom (blue, magenta, yellow) the figure shows the doublon density for $\gamma/U = 0.5, 1, 2$ in a three-dimensional cubic lattice with $J/U = 0.05$, $\bar{n} = 1$.

such as

$$\begin{aligned} \langle \hat{a}_i^\dagger \hat{a}_{i+1}\rangle = \frac{J}{U}\frac{2\tilde{n}^2(1-3n^d)^2U^2}{(1-3n^d)^2U^2+\gamma^2}(1-n^d) \\ \times\left\{1+e^{-\gamma t}\left[\frac{\gamma^2}{U^2}\cos(Ut)-\frac{\gamma}{U}\sin(Ut)\right]\right. \\ \left.+\,O\left(\frac{J}{U}\right)\right\}. \end{aligned} \tag{20}$$

These are plotted in Fig. 4 for typical parameters. As discussed above, two time scales are apparent in the graph.

V. LONG-WAVELENGTH MEASUREMENTS

We have explored so far the destruction of nonlocal correlations from the spontaneous localization of atoms to single lattice sites. As previously noted [19,35], the length scale of the localization is determined by the wavelength of the emitted light. Here we extend our argument to the case

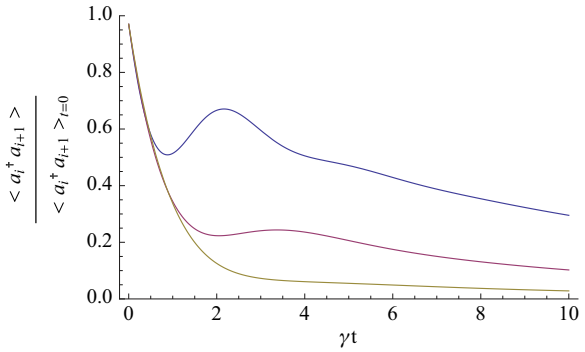

FIG. 4. (Color online) The evolution of the nearest-neighbor single-particle correlation function $\langle \hat{a}_i^\dagger \hat{a}_{i+1}\rangle$ in a Mott system. From top to bottom (blue, magenta, yellow) the figure shows the correlation for $\gamma = 0.5, 1, 2$ in a three-dimensional cubic lattice with $J = 0.05U$, $\bar{n} = 1$.

where the wavelength of light measuring the system is larger than the lattice spacing.

A simple model of such a measurement is

$$\hat{M}_i = \hat{n}_i^{\xi} = \frac{1}{\mathcal{N}_\xi} \sum_j e^{-\frac{1}{2}\left(\frac{r_j - r_i}{\xi}\right)^2} \hat{n}_j, \tag{21}$$

where the normalization $\mathcal{N}_\xi = \sum_i e^{-\frac{1}{2}(r_i/\xi)^2}$ is proportional to the width of the measurement.

Measurement with such long-wavelength light does not localize the atoms to single lattice sites. One learns less about the system but perturbs it proportionally less.

For free particles, the evolution of momentum states is replaced by the equation

$$\frac{d}{dt}\langle \hat{n}_k \rangle = -\frac{\mathcal{N}_{\xi/\sqrt{2}}}{(\mathcal{N}_\xi)^2}\gamma\left(\langle \hat{n}_k \rangle - \frac{1}{N_s}\sum G_\xi(p)\langle \hat{n}_{k+p}\rangle\right), \tag{22}$$

where $G_\xi(p) = \sum_i e^{-\frac{1}{4}\left(\frac{r_i}{\xi}\right)^2} e^{ipr_i}$. For the two-point correlation we find the closed form

$$\begin{aligned} \langle \hat{a}_i^\dagger \hat{a}_j \rangle &= \langle \hat{a}_i^\dagger \hat{a}_j \rangle_{t=0} e^{-\bar{\gamma}_{|i-j|}t}, \\ \bar{\gamma}_{|i-j|} &= g_\xi \sqrt{\frac{1}{\pi}}\frac{\Delta r}{2D\xi}\left\{1 - \exp\left[-\frac{1}{4}\left(\frac{r_i - r_j}{\xi}\right)^2\right]\right\}, \end{aligned} \tag{23}$$

where Δr is the spacing between sites and the function $g_\xi = \frac{\mathcal{N}_{\xi/\sqrt{2}}}{(\mathcal{N}_\xi)^2}\left[\sqrt{\frac{1}{\pi}}\frac{\Delta r}{2D\xi}\right]^{-1}$ has $g_\xi \approx 1$ for $|\xi| \gtrsim |\Delta r|$. Thus the rate at which correlations are lost is suppressed linearly in ξ and correlations on scales smaller than ξ decay at a much reduced rate.

VI. SUMMARY

We would like to have nondestructive site-resolved measurements. Unfortunately, no measurement is entirely nondestructive. Here we have quantified the effect of an ideal density measurement on a lattice system. In the superfluid regime, we use Bogoliubov theory to show that all spatial correlations decay exponentially with γt, the number of photons scattered. In the Mott regime, we find that the momenta of the quasiparticles are quickly scrambled, leading to a slowly evolving quasisteady state. In this slow-proliferation stage, fluctuations in the on-site density gradually grow. Similar physics was seen in numerical studies [18,20].

We predict how momentum occupation and single-particle correlations evolve with time. The former can be studied through time-of-flight experiments [36]. Protocols exist for the direct measurement of the single-particle correlation function [37–40]. Finally, though our focus is on measurement, the formalism and all of our results apply to spontaneous emission (in the absence of excitations to higher bands). As such they provide a quantitative estimate of the effects of spontaneous emission on coherence.

It is useful to put the loss of correlations into the context of the information gained as light is emitted. Assuming no dynamics, the continual measurement reduces the uncertainty in the number of atoms on a given site with time, $\delta n_i^2 \sim e^{-\gamma t}$ [41]. Thus, in the superfluid regime, the uncertainty falls at the same rate as do the correlations. In the Mott regime the uncertainty falls faster.

In this regard, long-wavelength measurements may be advantageous. If one wishes to measure the total number of particles in the cloud, the reduced uncertainty is set by the number of scattered photons, not their wavelength. As seen above, however, the backaction is reduced for long-wavelength probes. In general, one would wish to tailor the process of measurement so that all information carried by the probe is experimentally accessible.

ACKNOWLEDGMENTS

We thank Mukund Vengalattore and his students for extensive discussions. We acknowledge support from the US Army Research Office—Multidisciplinary University Research Initiative Nonequilibrium Many-Body Dynamics Grant No. 63834-PH-MUR.

APPENDIX: DERIVATION OF FORMULAS IN THE STRONGLY INTERACTING CASE

We present here the full derivation of our results for strongly interacting bosons.

Our starting point is the Hamiltonian

$$\begin{aligned} \hat{H}_{\mathrm{DH}} &= -J\sum_{\langle i,j\rangle}[\bar{n}(\bar{n}+1)\hat{d}_i^\dagger \hat{d}_j + \bar{n}\hat{h}_i^\dagger \hat{h}_j + \sqrt{\bar{n}(\bar{n}+1)}(\hat{d}_i^\dagger \hat{h}_j + \hat{h}_i^\dagger \hat{d}_j) + \mathrm{H.c.}] + U\sum_i(\hat{d}_i^\dagger \hat{d}_i + \hat{h}_i^\dagger \hat{h}_i) \\ &= \sum_k\left[\frac{U}{2} + J\left(\sqrt{\tilde{n}^2 + \frac{1}{4}} + \frac{1}{2}\right)\varepsilon_k\right]\hat{d}_k^\dagger \hat{d}_k + \left[\frac{U}{2} + J\left(\sqrt{\tilde{n}^2 + \frac{1}{4}} - \frac{1}{2}\right)\varepsilon_k\right]\hat{h}_k^\dagger \hat{h}_k + J\tilde{n}\varepsilon_k(\hat{d}_k \hat{h}_{-k} + \hat{h}_{-k}^\dagger \hat{d}_k^\dagger), \end{aligned} \tag{A1}$$

where, as before, $\varepsilon_k = -2\sum_{\Delta \boldsymbol{r}} \cos(\boldsymbol{k}\cdot\Delta\boldsymbol{r})$ and $\tilde{n} = \sqrt{\bar{n}(\bar{n}+1)}$. With this Hamiltonian the difference between the total number of doublons and holons is constant. We work in the commensurate case, where the particle density is given by the integer $\bar{n}$ and the total number of doublons equals the total number of holons.

The operators $\hat{d}_i$ and $\hat{h}_i$ have a hard-core constraint $\hat{d}_i^2 = \hat{h}_i^2 = \hat{d}_i\hat{h}_i = 0$. In equilibrium, at small J/U and T/U, this constraint has little effect as the densities of doublons and holons are small. During the measurement process, however, the number of quasiparticles grows, and we will need to include these constraints.

1. Initial state

The initial equilibrium properties of Eq. (A1) can be calculated by performing a Bogoliubov

transformation:

$$\begin{aligned}\hat{d}_k &= \cosh\theta_k \tilde{d}_k + \sinh\theta_k \tilde{h}^\dagger_{-k},\\ \hat{h}_k &= \cosh\theta_k \tilde{h}_k + \sinh\theta_k \tilde{d}^\dagger_{-k},\\ \tanh(2\theta_k) &= -\frac{2J\tilde{n}\varepsilon_k}{U + 2J\sqrt{\tilde{n}^2 + \frac{1}{4}\varepsilon_k}}.\end{aligned} \tag{A2}$$

Neglecting the hard-core constraints, which can be ignored for low-defect densities, $\tilde{d}_k$ and $\tilde{h}_k$ are bosonic operators and the Hamiltonian takes the diagonal form:

$$\begin{aligned}\hat{H}_{\rm DHB} &= \sum_k \left(\tilde{E}_k + \frac{1}{2}J\varepsilon_k\right)\tilde{d}^\dagger_k\tilde{d}_k + \left(\tilde{E}_k - \frac{1}{2}J\varepsilon_k\right)\tilde{h}^\dagger_k\tilde{h}_k,\\ \tilde{E}_k &= \frac{1}{2}\sqrt{\left(U + 2J\sqrt{\tilde{n}^2 + \frac{1}{4}\varepsilon_k}\right)^2 - (2J\tilde{n}\varepsilon_k)^2}.\end{aligned} \tag{A3}$$

We take our initial conditions to correspond to the ground state, where $\langle\tilde{d}^\dagger_k\tilde{d}_k\rangle = \langle\tilde{h}^\dagger_k\tilde{h}_k\rangle = 0$, and hence

$$\begin{aligned}\langle\hat{d}^\dagger_k\hat{d}_k\rangle_{t=0} &= \langle\hat{h}^\dagger_k\hat{h}_{-k}\rangle_{t=0} = \left(\frac{J}{U}\right)^2\tilde{n}^2\varepsilon_k^2 + O\left(\frac{J}{U}\right)^3,\\ \langle\hat{d}_k\hat{h}_{-k}\rangle_{t=0} &= -\frac{J}{U}\tilde{n}\varepsilon_k + O\left(\frac{J}{U}\right)^2.\end{aligned} \tag{A4}$$

The calculation may be easily extended to low finite temperatures as long as the initial particle densities remain of the order $(\frac{J}{U})^2$.

2. Evolution equations

To obtain the full evolution equations we must now include the hard-core constraints. In momentum space, these constraints lead to the commutation relations

$$\begin{aligned}[\hat{d}_k,\hat{d}^\dagger_q] &= \delta_{k,q} - \frac{1}{N_s}\sum_p 2\hat{d}^\dagger_{q+p}\hat{d}_{k+p} + \hat{h}^\dagger_{q+p}\hat{h}_{k+p},\\ [\hat{h}_k,\hat{h}^\dagger_q] &= \delta_{k,q} - \frac{1}{N_s}\sum_p \hat{d}^\dagger_{q+p}\hat{d}_{k+p} + 2\hat{h}^\dagger_{q+p}\hat{h}_{k+p},\\ [\hat{d}_k,\hat{h}^\dagger_q] &= -\frac{1}{N_s}\sum_p \hat{h}^\dagger_{q+p}\hat{d}_{k+p}.\end{aligned} \tag{A5}$$

In these sums, the terms where operators have different momentum indices will add incoherently, suggesting the approximation

$$\begin{aligned}[\hat{d}_k,\hat{d}^\dagger_q] &\approx \delta_{k,q}(1 - 2\hat{n}^d - \hat{n}^h),\\ [\hat{h}_k,\hat{h}^\dagger_q] &\approx \delta_{k,q}(1 - 2\hat{n}^h - \hat{n}^d),\\ [\hat{d}_k,\hat{h}^\dagger_q] &\approx 0,\end{aligned} \tag{A6}$$

where $\hat{n}^d = \frac{1}{N_s}\sum_k \hat{d}^\dagger_k\hat{d}_k$ and similarly for $\hat{n}^h$.

We substitute Eq. (A1) into Eq. (3), using the commutators in Eq. (A6), for $\hat{O} = \hat{d}^\dagger_k\hat{d}_k$ and $\hat{d}_k\hat{h}_{-k}$. We assume that the total number of quasiparticles is uncorrelated with their momentum distribution:

$$\begin{aligned}\langle\hat{n}^d\hat{d}^\dagger_k\hat{d}_k\rangle &\approx n^d\langle\hat{d}^\dagger_k\hat{d}_k\rangle,\\ \langle\hat{n}^d\hat{h}^\dagger_k\hat{h}_k\rangle &\approx n^d\langle\hat{h}^\dagger_k\hat{h}_k\rangle,\\ \langle\hat{n}^d\hat{d}_k\hat{h}_{-k}\rangle &\approx n^d\langle\hat{d}_k\hat{h}_{-k}\rangle,\\ \langle\hat{n}^h\hat{d}^\dagger_k\hat{d}_k\rangle &\approx n^h\langle\hat{d}^\dagger_k\hat{d}_k\rangle,\\ \langle\hat{n}^h\hat{h}^\dagger_k\hat{h}_k\rangle &\approx n^h\langle\hat{h}^\dagger_k\hat{h}_k\rangle,\\ \langle\hat{n}^h\hat{d}_k\hat{h}_{-k}\rangle &\approx n^h\langle\hat{d}_k\hat{h}_{-k}\rangle,\end{aligned} \tag{A7}$$

where $n^{d,h} = \langle\hat{n}^{d,h}\rangle$. One can formally derive these relations through perturbation theory in J/U, although their validity is wider.

The evolution equations then simplify to a set of coupled nonlinear differential equations:

$$\begin{aligned}\frac{d}{dt}\langle\hat{d}^\dagger_k\hat{d}_k\rangle &= -2\tilde{n}\bar{J}_t\varepsilon_k{\rm Im}[\langle\hat{d}_k\hat{h}_{-k}\rangle] - \gamma(\langle\hat{d}^\dagger_k\hat{d}_k\rangle - n^d),\\ \frac{d}{dt}\langle\hat{d}_k\hat{h}_{-k}\rangle &= -i\tilde{n}\bar{J}_t\varepsilon_k P_t - i\left(\bar{U}_t + 2\sqrt{\tilde{n}^2 + \frac{1}{4}}\bar{J}_t\varepsilon_k\right)\langle\hat{d}_k\hat{h}_{-k}\rangle\\ &\quad - \gamma\langle\hat{d}_k\hat{h}_{-k}\rangle,\end{aligned} \tag{A8}$$

where all k dependence is through $\varepsilon_k = -2\sum_{\Delta\boldsymbol{r}}\cos(\boldsymbol{k}\cdot\Delta\boldsymbol{r})$. Here

$$\begin{aligned}\bar{J}_t &= J(1 - 3n^d),\\ \bar{U}_t &= U(1 - 3n^d),\\ P_t &= (1 + 2\langle\hat{d}^\dagger_k\hat{d}_k\rangle - 3n^d)\end{aligned} \tag{A9}$$

are time dependent but, as we will see, vary at a rate much slower than γ.

In the commensurate case, $n^d = n^h$, and one finds identical initial values and evolution equations for the momentum occupation of holons and doublons, hence $\langle\hat{d}^\dagger_k\hat{d}_k\rangle = \langle\hat{h}^\dagger_k\hat{h}_k\rangle$ at all times.

3. Ansatz solution

All of the k dependence in Eq. (A8) arises from terms of the form $J\varepsilon_k$. Since $J \ll U$, we can expand in this product, finding

$$\begin{aligned}\langle\hat{d}^\dagger_k\hat{d}_k\rangle &= \langle\hat{h}^\dagger_{-k}\hat{h}_{-k}\rangle = dd^{(0)} + dd^{(2)}\left(\frac{J}{U}\right)^2\varepsilon_k^2 + O\left(\frac{J}{U}\right)^3,\\ \langle\hat{d}_k\hat{h}_{-k}\rangle &= dh^{(1)}\left(\frac{J}{U}\right)\varepsilon_k + O\left(\frac{J}{U}\right)^2,\end{aligned} \tag{A10}$$

where $dd^{(0)}, dd^{(2)}, dh^{(1)}$ are functions of time but not k. By Fourier transforming these expressions we can relate them to the more familiar

$$\begin{aligned}n^d &= dd^{(0)} + 2D\left(\frac{J}{U}\right)^2 dd^{(2)} + O\left(\frac{J}{U}\right)^3,\\ \langle\hat{d}_i\hat{h}_{i+1}\rangle &= -\frac{J}{U}dh^{(1)} + O\left(\frac{J}{U}\right)^2.\end{aligned} \tag{A11}$$

Equations (A8) then reduce to

$$\frac{d}{dt}n^d = \left(\frac{J}{U}\right)4D\tilde{n}\bar{J}_t\mathrm{Im}\left[\langle\hat{d}_i\hat{h}_{i+1}\rangle/\frac{J}{U}\right] + O\left(\frac{J^3}{U^2}\right), \tag{A12}$$

$$\frac{d}{dt}\langle\hat{d}_i\hat{h}_{i+1}\rangle = i\tilde{n}\bar{J}_t(1-n^d) - i\bar{U}_t\langle\hat{d}_i\hat{h}_{i+1}\rangle - \gamma\langle\hat{d}_i\hat{h}_{i+1}\rangle + O\left(\frac{J^2}{U}\right), \tag{A13}$$

$$\frac{d}{dt}dd^{(2)} = 2\tilde{n}\bar{U}_t\mathrm{Im}\left[\langle\hat{d}_i\hat{h}_{i+1}\rangle/\frac{J}{U}\right] - \gamma dd^{(2)} + O(J), \tag{A14}$$

while the initial conditions are

$$n^d_{t=0} = \left(\frac{J}{U}\right)^2 2D\tilde{n}^2, \quad dd^{(2)}_{t=0} = \tilde{n}^2, \quad \langle\hat{d}_i\hat{h}_{i+1}\rangle_{t=0} = \frac{J}{U}\tilde{n}. \tag{A15}$$

We note that Eqs. (A12) and (A13) are coupled to each other but independent of Eq. (A14). At this point, the equations may be numerically integrated for any given values of γ, J, U. Typical values are plotted in Figs. 3 and 4.

4. Short-time behavior

The initial and short-time behavior of Eqs. (A12) and (A13) can be analyzed using $n^d_{t=0} \sim (\frac{J}{U})^2$. Thus, we can neglect the nonlinear terms, $\bar{J}_t \approx J, \bar{U}_t \approx U$, finding

$$\frac{d}{dt}n^d = \frac{J}{U}4D\tilde{n}J\ \mathrm{Im}\left[\langle\hat{d}_i\hat{h}_{i+1}\rangle/\frac{J}{U}\right] + O\left(\frac{J^3}{U^2}, n^d\right),$$

$$\frac{d}{dt}\langle\hat{d}_i\hat{h}_{i+1}\rangle = i\tilde{n}J - iU\langle\hat{d}_i\hat{h}_{i+1}\rangle - \gamma\langle\hat{d}_i\hat{h}_{i+1}\rangle + O\left(\frac{J^2}{U}, n^d\right). \tag{A16}$$

The second equation produces a function which oscillates with frequency U while decaying at a rate γ to a steady-state value:

$$\langle\hat{d}_i\hat{h}_{i+1}\rangle = \left[\langle\hat{d}_i\hat{h}_{i+1}\rangle_{t=0} - \frac{iJ\tilde{n}}{iU+\gamma}\right]e^{-\gamma t}e^{-iUt} + \frac{iJ\tilde{n}}{iU+\gamma}. \tag{A17}$$

Using this result to calculate the number of doublons, we find

$$n^d = n^d_{t=0} + \frac{4D\tilde{n}^2J^2}{U^2+\gamma^2}\left(\gamma t - \frac{2\gamma^2}{U^2+\gamma^2} \times \left\{1 - e^{-\gamma t}\left[\cos(Ut) - \frac{1}{2}\left(\frac{U}{\gamma} - \frac{\gamma}{U}\right)\sin(Ut)\right]\right\}\right). \tag{A18}$$

Aside from small transients, we see a linear increase in n^d with characteristic rate $1/\tau_p = \frac{4D\tilde{n}^2J^2}{U^2+\gamma^2}\gamma$. Physically, this is the rate at which virtual doublon-holon pairs are imaged. This linearized theory breaks down when $n^d \sim 1$. Thus it is valid until $t \sim \tau_p \gg 1/\gamma$.

5. General behavior

Given the separation of time scales between the rate of change in n^d and $\langle\hat{d}_i\hat{h}_{i+1}\rangle$, we can adiabatically eliminate the nonlinear terms in Eq. (A12), rather than simply neglecting them. This yields

$$\langle\hat{d}_i\hat{h}_{i+1}\rangle = (\langle\hat{d}_i\hat{h}_{i+1}\rangle_{t=0} - \langle\hat{d}_i\hat{h}_{i+1}\rangle^{\mathrm{long}})e^{-\gamma t}e^{-iUt} + \langle\hat{d}_i\hat{h}_{i+1}\rangle^{\mathrm{long}} + O\left(\frac{J}{U}\right)^2, \tag{A19}$$

$$\langle\hat{d}_i\hat{h}_{i+1}\rangle^{\mathrm{long}} = \frac{i\tilde{n}J(1-3n^d)}{iU(1-3n^d)+\gamma}(1-n^d)$$

at all times. When $n^d \ll 1$, this reduces to Eq. (A17).

Substituting this into Eq. (A12) yields

$$\frac{d}{dt}n^d = \frac{J^2}{U^2}\frac{4D\tilde{n}^2(1-3n^d)^2U^2}{(1-3n^d)^2U^2+\gamma^2}(1-n^d)\gamma \times \left\{1 - e^{-\gamma t}\left[\cos(Ut) + \frac{\gamma}{U}\sin(Ut)\right]\right\}, \tag{A20}$$

which simplifies to Eq. (A16) for $n^d \ll 1$. Likewise, we adiabatically eliminate Eq. (A14) to obtain Eq. (18).

[1] K. D. Nelson, X. Li, and D. S. Weiss, Nature Phys. **3**, 556 (2007).
[2] T. Gericke, P. Würtz, D. Reitz, T. Langen, and H. Ott, Nature Phys. **4**, 949 (2008).
[3] W. S. Bakr, J. I. Gillen, A. Peng, S. Fölling, and M. Greiner, Nature (London) **462**, 74 (2009).
[4] J. F. Sherson, C. Weitenberg, M. Endres, M. Cheneau, I. Bloch, and S. Kuhr, Nature (London) **467**, 68 (2010).
[5] Y. S. Patil, L. M. Aycock, S. Chakram, and M. Vengalattore, arXiv:1404.5583v1.
[6] A. Naik, O. Buu, M. D. LaHaye, A. D. Armour, A. Clerk, M. P. Blencowe, and K. C. Schwab, Nature (London) **443**, 193 (2006).
[7] G. Barontini, R. Labouvie, F. Stubenrauch, A. Vogler, V. Guarrera, and H. Ott, Phys. Rev. Lett. **110**, 035302 (2013).
[8] A. G. Fowler, M. Mariantoni, J. M. Martinis, and A. N. Cleland, Phys. Rev. A **86**, 032324 (2012).
[9] W. M. Itano, D. J. Heinzen, J. J. Bollinger, and D. J. Wineland, Phys. Rev. A **41**, 2295 (1990).
[10] M. C. Fischer, B. Gutiérrez-Medina, and M. G. Raizen, Phys. Rev. Lett. **87**, 040402 (2001).
[11] F. Schäfer, I. Herrera, S. Cherukattil, C. Lovecchio, F. S. Cataliotti, F. Caruso, and A. Smerzi, Nature Commun. **5**, 3194 (2014).

[12] D. A. R. Dalvit, J. Dziarmaga, and R. Onofrio, Phys. Rev. A **65**, 033620 (2002).
[13] V. Giovannetti, S. Lloyd, and L. Maccone, Science **306**, 1330 (2004).
[14] M. Hatridge, S. Shankar, M. Mirrahimi, F. Schackert, K. Geerlings, T. Brecht, K. M. Sliwa, B. Abdo, L. Frunzio, S. M. Girvin *et al.*, Science **339**, 178 (2013).
[15] J. Gambetta, A. Blais, M. Boissonneault, A. A. Houck, D. I. Schuster, and S. M. Girvin, Phys. Rev. A **77**, 012112 (2008).
[16] J. J. Mendoza-Arenas, T. Grujic, D. Jaksch, and S. R. Clark, Phys. Rev. B **87**, 235130 (2013).
[17] D. A. R. Dalvit, J. Dziarmaga, and R. Onofrio, Phys. Rev. A **65**, 053604 (2002).
[18] D. Poletti, J.-S. Bernier, A. Georges, and C. Kollath, Phys. Rev. Lett. **109**, 045302 (2012).
[19] H. Pichler, A. J. Daley, and P. Zoller, Phys. Rev. A **82**, 063605 (2010).
[20] D. Poletti, P. Barmettler, A. Georges, and C. Kollath, Phys. Rev. Lett. **111**, 195301 (2013).
[21] H. Pichler, J. Schachenmayer, A. J. Daley, and P. Zoller, Phys. Rev. A **87**, 033606 (2013).
[22] Z. Cai and T. Barthel, Phys. Rev. Lett. **111**, 150403 (2013).
[23] J. Schachenmayer, L. Pollet, M. Troyer, and A. J. Daley, Phys. Rev. A **89**, 011601 (2014).
[24] S. Diehl, A. Micheli, A. Kantian, B. Kraus, H. P. Büchler, and P. Zoller, Nature Phys. **4**, 878 (2008).
[25] I. B. Mekhov and H. Ritsch, J. Phys. B **45**, 102001 (2012).
[26] F. Gerbier and Y. Castin, Phys. Rev. A **82**, 013615 (2010).
[27] I. Vidanovic, D. Cocks, and W. Hofstetter, arXiv:1402.0011v1.
[28] M. Knap, D. A. Abanin, and E. Demler, Phys. Rev. Lett. **111**, 265302 (2013).
[29] J.-F. Riou, L. A. Zundel, A. Reinhard, and D. S. Weiss, arXiv:1311.0073v1.
[30] P. Barmettler and C. Kollath, Phys. Rev. A **84**, 041606 (2011).
[31] P. Hohenberg and P. Martin, Ann. Phys. (NY) **34**, 291 (1965).
[32] C. W. Gardiner, *Handbook of Stochastic Methods*, 2nd ed. (Springer-Verlag, Berlin, 1985).
[33] A. Griffin, Phys. Rev. B **53**, 9341 (1996).
[34] P. Barmettler, D. Poletti, M. Cheneau, and C. Kollath, Phys. Rev. A **85**, 053625 (2012).
[35] M. Holland, S. Marksteiner, P. Marte, and P. Zoller, Phys. Rev. Lett. **76**, 3683 (1996).
[36] K. B. Davis, M.-O. Mewes, M. R. Andrews, N. J. van Druten, D. S. Durfee, D. M. Kurn, and W. Ketterle, Phys. Rev. Lett. **75**, 3969 (1995).
[37] Z. Hadzibabic, P. Krüger, M. Cheneau, B. Battelier, and J. Dalibard, Nature (London) **441**, 1118 (2006).
[38] S. Richard, F. Gerbier, J. H. Thywissen, M. Hugbart, P. Bouyer, and A. Aspect, Phys. Rev. Lett. **91**, 010405 (2003).
[39] J. Stenger, S. Inouye, A. P. Chikkatur, D. M. Stamper-Kurn, D. E. Pritchard, and W. Ketterle, Phys. Rev. Lett. **82**, 4569 (1999).
[40] E. Hagley, L. Deng, M. Kozuma, M. Trippenbach, Y. Band, M. Edwards, M. Doery, P. Julienne, K. Helmerson, S. Rolston *et al.*, Phys. Rev. Lett. **83**, 3112 (1999).
[41] P. Gregory, in *Bayesian Logical Data Analysis for the Physical Sciences: A Comparative Approach with Mathematica Support* (Cambridge University, Cambridge, 2005), Chap. 14, pp. 376–388.